



Drastically enhanced visible-light photocatalytic degradation of colorless aromatic pollutants over TiO₂ via a charge-transfer-complex path: A correlation between chemical structure and degradation rate of the pollutants

Nan Wang^a, Lihua Zhu^{a,*}, Yingping Huang^b, Yuanbin She^c, Yanmin Yu^c, Heqing Tang^{a,*}

^a College of Chemistry and Chemical Engineering, Huazhong University of Science and Technology, Wuhan 430074, PR China

^b Chemistry and Life Science College, China Three Gorges University, Yichang 443002, PR China

^c College of Environmental and Energy Engineering, Beijing University of Technology, Beijing 100124, PR China

ARTICLE INFO

Article history:

Received 8 February 2009

Revised 18 May 2009

Accepted 5 June 2009

Available online 22 July 2009

Keywords:

Titanium dioxide

Charge-transfer

Surface complex

Visible-light irradiation

Degradation

ABSTRACT

Photocatalytic degradation of colorless aniline and phenolic pollutants was investigated over TiO₂ under visible-light irradiation, which was confirmed to proceed via a charge-transfer-complex (CTC)-mediated pathway. The correlation between the chemical structure and the degradation rate of these pollutants was established experimentally and theoretically. It was found that an electron-donating substituent in benzene ring, which raises the highest occupied molecular orbital and lowers the ionization potential of the organic compound, is favorable to the CTC-mediated photodegradation of the pollutant, but an electron-withdrawing substituent has a reversed effect. The addition of sacrificial electron acceptors was adopted to enhance the degradation and mineralization of the aromatic pollutants. The increased degradation rate by 3 to 10 times suggests that the CTC-mediated photocatalytic technique has promising applications in the removal of colorless organic pollutants in the presence of sacrificial electron acceptors.

© 2009 Elsevier Inc. All rights reserved.

1. Introduction

TiO₂ photocatalysis has been intensively investigated for the elimination of environmental toxic pollutants [1–8]. However, the neat TiO₂ photocatalyst can only make use of UV radiation, less than 5% of solar energy, as determined by its high band-gap energy of 3.2 eV ($\lambda < 387$ nm). Thus, a great deal of efforts has been devoted to improve the intrinsic efficiency of TiO₂ under the visible light by modifying the TiO₂ photocatalysts with various methods such as depositing noble metals [2], using composite semiconductors [3], coating a thin layer of polyaniline [4], and doping with metals [5,6], nonmetals [9,10], and multiple elements [11,12].

Rather than the modification of TiO₂ photocatalyst, another important approach to utilize solar radiation focuses on the inherent organic pollutants. An example is the self-sensitized degradation of dyes under the visible irradiation, whereby the dye molecule absorbs a photon of visible light and then enters its excited state, from which an electron is injected into the conduction band of TiO₂ [13,14]. Unlike the dye-induced visible-light TiO₂ photocatalysis, Agrios et al. observed that 2,4,5-trichlorophenol was transformed to coupling products such as hexachlorodibenzo-*p*-dioxin over Degussa P25 having mixed phases

of anatase and rutile under visible light and they ascribed the visible-light reactivity to a charge-transfer-complex (CTC) mechanism, in which neither the photocatalyst nor the organic compound absorbs visible light by itself [15,16]. Kim and Choi reported that phenolic compounds were degraded in anatase TiO₂ suspensions under visible irradiation via a CTC-mediated path, and observed that the reactivity of different TiO₂ photocatalysts was correlated with their surface area [17]. Similar phenomena were observed in the visible-light-induced TiO₂ photocatalysis of fluoroquinolone antibacterial agents by Paul and co-workers [18]. Li et al. found that anatase TiO₂ nanoparticles showed higher visible-light photocatalytic activity for phenolic compounds than P25 did, possibly due to the formation of surface complexes between TiO₂ and the organic substrates, and between TiO₂ and the degradation intermediates [19]. The CTC-mediated photocatalytic degradation over TiO₂ under visible irradiation is greatly important for the removal of colorless pollutants in the natural environment, but the correlation between the efficiency of photocatalytic degradation and the chemical structure of the colorless pollutants is not yet known. We have found that the above-mentioned examples share a similarity in that the substrates contain phenolic and/or carboxylic acid groups, which are beneficial to the complex formation, but the reason for the different reactivities of these analog is not clearly understood yet. We have also noted that the CTC-mediated photocatalytic efficiency is not so high to satisfy the practical application in the removal of the colorless organic pollutants under

* Corresponding authors. Fax: +86 27 87543632.

E-mail addresses: lhzhu62@yahoo.com.cn (L. Zhu), hqtang62@yahoo.com.cn (H. Tang).

sunlight. For example, it was reported that no mineralization was accompanied by the photodegradation of ciprofloxacin or 2,4,5-trichlorophenol, and only 25% of the initial 4-chlorophenol was mineralized within 10 h under visible irradiation [15–18]. The little mineralization indicates that the degradation byproducts of the parent compounds cannot be further degraded via a CTC-mediated path under visible-light irradiation.

The goals of the present work are to understand the structure-reactivity correlation in the visible-light photocatalytic degradation of colorless aromatic pollutants and to improve the overall photocatalytic efficiency in the CTC-mediated path by in situ adding appropriate electron acceptors. Thus, benzene derivatives containing various functional groups such as amino, hydroxyl, and carboxyl groups were selected as model compounds to be photodegraded, and various additives (such as Cu^{2+} , H_2O_2 , Cr(VI) , BrO_3^-) were selected as external electron scavengers. It was anticipated that the addition of appropriate electron acceptors could significantly increase the degradation and mineralization of colorless organic pollutants with favorable function groups via CTC-mediated path, as a promising approach for the photocatalytic removal of colorless organic pollutants under the visible irradiation.

2. Experimental section

2.1. Materials

Anatase TiO_2 powders (BET area of $180.9 \text{ m}^2 \text{ g}^{-1}$ [8]) and P25 powders (BET area, $49.6 \text{ m}^2 \text{ g}^{-1}$, anatase 80%, rutile 20% [17,18]) were obtained from Zhoushan Nano Company (China) and Degussa, respectively. In the preliminary experiments, we confirmed that pure anatase TiO_2 powders showed a better visible-light activity than P25. For example, the apparent photodegradation rate constant of salicylic acid was $1.4 \times 10^{-3} \text{ min}^{-1}$ over anatase TiO_2 , being ca. 2 times greater than that ($0.5 \times 10^{-3} \text{ min}^{-1}$) on P25. Thus, only the anatase TiO_2 powders were used as the photocatalyst in the present work. Aniline was freshly distilled under reduced pressure and stored at low temperature prior to use. All other reagents were of analytical reagent grade and were used as received. Distilled water was used throughout the experiment. Solution pH was adjusted using diluted H_2SO_4 and NaOH solutions. The very small addition of the added anions and cations was experimentally confirmed to have no marked effects on the results in the present work.

2.2. Photoreactor and light source

A 500-W halogen lamp was positioned inside a cylindrical Pyrex vessel surrounded by a circulating water jacket (Pyrex) to cool the lamp. A cutoff filter was placed outside the Pyrex jacket to completely remove any radiation below 420 nm.

2.3. Procedure and analyses

For typical photocatalytic runs, TiO_2 (0.05 g) was suspended into 50 mL aqueous solution of organic compounds (0.1 mM) with or without the addition of specified electron acceptor (such as $\text{Cr}_2\text{O}_7^{2-}$, 0.1 mM), followed by adjusting pH to 3.0, because our preliminary experiments indicated that the photodegradation rates of tested organics were highest at pH 3.0 in the pH range from 2.0 to 5.0. Prior to irradiation, the suspension was first sonicated for 60 s, and then magnetically stirred in the dark for ca. 30 min to ensure the establishment of adsorption–desorption equilibrium of the concerned compounds on TiO_2 surface. The concentration of organic compounds after equilibration was measured and was taken as the initial concentration (c_0), to discount the adsorption in the

dark. The reaction mixture was maintained in suspension by using a magnetic stirrer before and during the irradiation.

At appropriate time intervals, 2 mL aliquots were sampled, immediately centrifuged at 14,000 rpm for 15 min, and then filtered through a $0.22\text{-}\mu\text{m}$ pore size filter to remove the TiO_2 particles. The filtrates were collected and analyzed. The degradation of organic compounds was quantified by high-performance liquid chromatographer (JASCO PU-2089) equipped with a UV detector (JASCO UV-2075) and a Waters Xterra C18 ODS column ($4.6 \times 150 \text{ mm}$). The mobile phase was 45% methanol and 55% KH_2PO_4 buffer (0.01 M) at 0.8 mL min^{-1} . The concentration of Cr(VI) was determined by using the diphenyl carbazide colorimetric method at 540 nm (GB 7466-87, Standards of China) on a Cary 50 UV-vis spectrophotometer (Varian). Organic carbon mineralization was measured on a TOC analyzer (Analytika jena, Germany). The produced formic acid as intermediate was quantified by ion chromatography on a Dionex DX-500 IC system with an ED-40 electrochemical detector operating in conductivity mode and an IonPac ICE-AS14 column. Triplicate runs were carried out for each test, and the obtained relative standard deviation was generally less than 5%.

The interaction between organic compounds and TiO_2 surface was examined by diffuse reflectance UV-vis spectroscopy (DRS). The samples were prepared as follows: TiO_2 (0.20 g) was dispersed in 50 mL aqueous solutions of 0.1 mM organic compounds with or without the addition of 0.1 mM $\text{Cr}_2\text{O}_7^{2-}$. After the TiO_2 suspensions were stirred for 24 h in dark, the powders were collected by vacuum filtration with a filter ($0.22\text{-}\mu\text{m}$) and dried in dark at room temperature. Their DRS spectra were measured on a UV-2550 spectrometer (Shimadzu), with BaSO_4 as a standard.

2.4. Computational methods

The energies of the highest occupied molecular orbital (HOMO) E_{HOMO} and vertical ionization potential (VIP) of benzene derivatives were calculated by using the Amsterdam Density Functional (ADF) program package ADF2007.01 [20]. The Slater-type orbitals (STOs) basis set employed is the standard ADF-TZP, which is triple- ζ for valence orbitals plus one polarization function. The exchange-correlation potential is based on the Vosko-Wilk-Nusair (VWN) [21] local density functional plus the PW91 [22] generalized gradient approximations (GGAs).

3. Results and discussion

3.1. CTC-mediated photocatalytic degradation of colorless organic pollutants

At first, it was experimentally confirmed that both the adsorption of the tested organics on TiO_2 surface and their direct photolysis under visible light were negligible. For example, a 300-min visible irradiation converted only 0.2% of the added salicylic acid (0.1 mM) in TiO_2 -free solution, and a 300-min treatment in TiO_2 dispersions but without the visible illumination produced a conversion of less than 2.0% for salicylic acid. Fig. 1 illustrates the photocatalytic degradation of different organics in TiO_2 suspensions irradiated by visible light. It is observed that although benzoic acid is hardly degraded, phenol, *p*-hydroxybenzoic acid and salicylic acid can be degraded slowly (Fig. 1a), and the degradation of the later three organic pollutants is much promoted by the addition of a small amount of Cr(VI) (Fig. 1b). Because the photooxidation of salicylic acid in TiO_2 -free Cr(VI) -containing solution under visible irradiation is almost not observable (Curve 5 in Fig. 1b), the enhancing effect of Cr(IV) addition is indeed attributed to the accelerated photocatalytic degradation of the concerned organic

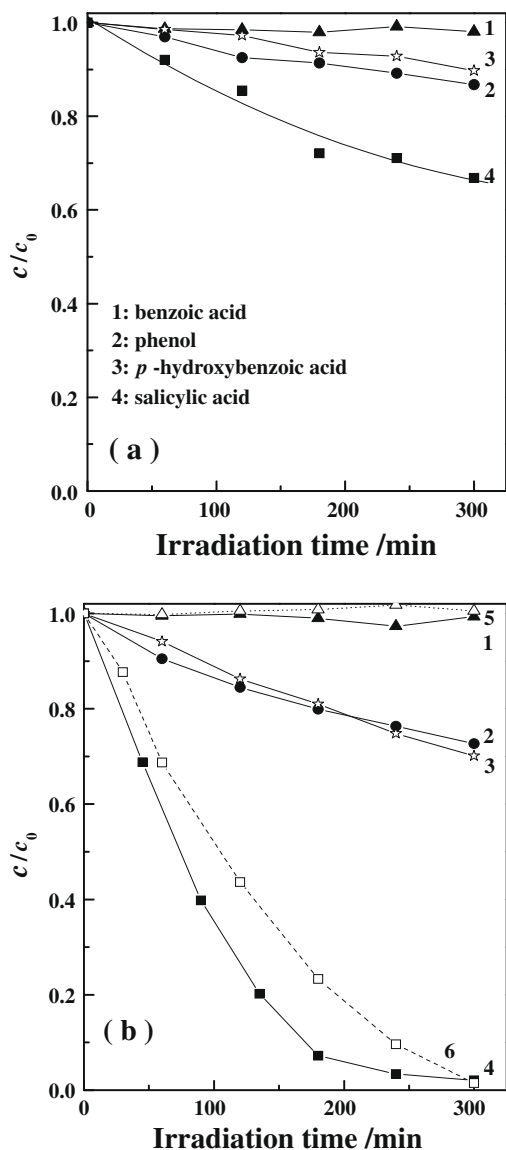


Fig. 1. Visible-light photocatalytic degradation of several organic pollutants (0.1 mM) over TiO_2 (1.0 g L^{-1}) in the absence (a) and presence (b) of $0.1 \text{ mM Cr}_2\text{O}_7^{2-}$ at pH 3.0. As a control, curves 5 and 6 in (b) present the photooxidation of salicylic acid in TiO_2 -free Cr(VI) -containing solution and the photoreduction of Cr(VI) over TiO_2 in the mixture of salicylic acid and Cr(VI) under visible irradiation, respectively.

pollutants. Here, it is worthy noting that the reason for the use of Cr(VI) as an additive to increase the photocatalytic degradation of the colorless aromatic pollutants is only the operational easiness in the monitoring of the Cr(VI) concentrations during the photocatalysis, although the simultaneous removal of both the organic pollutants and the inorganic pollutant (Cr(VI)) is also the focus of many researches reported in the literature [8,23,24]. The effects of other additives for promoting the visible-light photodegradation of the aromatics will be discussed in more detail along with other sacrificial electron acceptors in Section 3.3.

The degradation of the tested pollutants generally obeys a pseudo first order reaction in kinetics, which can be expressed as $\ln(c_t/c_0) = -kt$, and the apparent rate constant k is shown in Table 1. In the Cr(VI) -free suspensions, the k value is increased in the order of salicylic acid ($1.40 \times 10^{-3} \text{ min}^{-1}$) > phenol ($0.46 \times 10^{-3} \text{ min}^{-1}$), *p*-hydroxybenzoic acid ($0.36 \times 10^{-3} \text{ min}^{-1}$). When Cr(VI) is added into the suspensions, k is correspondingly increased by a factor

of 3 to 10 times in the order of salicylic acid ($14.0 \times 10^{-3} \text{ min}^{-1}$) > *p*-hydroxybenzoic acid ($1.2 \times 10^{-3} \text{ min}^{-1}$), phenol ($1.0 \times 10^{-3} \text{ min}^{-1}$). Because neither TiO_2 nor the tested organic pollutants have absorptions in the visible region, the photocatalytic degradation of these organic pollutants should be attributed to a CTC-mediated photocatalytic process. If it is true, a surface complex will be formed on the surface of the pollutant-adsorbed TiO_2 nanoparticles.

The DRS spectra were measured to evidence the electronic interaction between organic substrates and TiO_2 in the absence and presence of Cr(VI) , as shown in Fig. 2. It can be easily seen that pure TiO_2 itself cannot absorb visible light (curve 1 in Fig. 2a), indicating that TiO_2 is active only under UV light irradiation as expected. In contrast, once the organic pollutant is adsorbed on TiO_2 surface, the DRS spectrum is red shifted into the visible region (curves 2 to 6 in Fig. 2a), implying the existence of the intramolecular ligand-to-titanium charge-transfer (LMCT) transition within the surface complexes [25–27]. Either phenol or salicylic acid can form a charge transfer complex on TiO_2 surface, which shows an absorption band near 420 nm, being assigned to the LMCT transition within the surface complexes [25]. When the complex absorbs photons of visible light, the photo-induced electrons can be directly transferred from the HOMO of the organic compound to TiO_2 conduction band (CB) and then delivered to O_2 , resulting in the oxidation of the organics to radical cations (R^{\bullet}) and the reduction of O_2 to $\text{O}_2^{\bullet -}$. The R^{\bullet} radical is further converted to intermediates by a series of electron transfers, addition of O_2 and/or reacting with $\text{O}_2^{\bullet -}$, thereby inducing the degradation of organics. This process proceeds with a CTC-mediated path, which may provide an approach to degrade colorless organic pollutants over TiO_2 under visible-light irradiation. It is also noted that the co-existence of Cr(VI) increases significantly the absorption of the corresponding pollutant-adsorbed TiO_2 systems at $\lambda > 420 \text{ nm}$ (Fig. 2b), partially due to the absorption of Cr(VI) itself (curve 7 in Fig. 2b). It seems that the enhanced absorption of the CTC in the presence of Cr(VI) results in the promoted photocatalytic degradation of the organic pollutants. However, when the background absorption of Cr(VI) is subtracted from the absorption of the organic pollutant/ Cr(VI) / TiO_2 system, the Cr(VI) -induced increasing effect in the absorption in the visible region is much weaker than the increasing effect in the visible-light photocatalytic degradation of these pollutants. Therefore, the significantly increased photocatalytic degradation of these pollutants under visible irradiation in the presence of Cr(VI) is not primarily due to the increased absorption to the visible light, but due to the function of Cr(VI) as an electron scavenger, which markedly depresses the backward recombination of photo-injected electrons in TiO_2 CB with the adsorbed R^{\bullet} radical via the CTC-mediated path.

Here, it is worthy noting that Irie and coworkers recently reported Cr(III) -grafted TiO_2 as a novel visible-light-sensitive efficient photocatalyst [28]. The Cr(III) -grafted TiO_2 was demonstrated to be able to decompose 2-propanol into CO_2 via acetone under visible-light (450 to 580 nm) irradiation, and the reaction was explained by the formation of pseudo metal to metal charge transfer induced by visible light, that is, the electron in Cr(III) was directly injected into the CB of TiO_2 , leading to the formation of Cr(VI) . We have recently investigated the simultaneous photocatalytic reduction of Cr(VI) and photocatalytic oxidation of organics on TiO_2 under UV irradiation, and found that some Cr(III) species are deposited on the surface of TiO_2 nanoparticles after a fairly long period of irradiation time [29]. In the present work, we do not intend to study the reduction of Cr(VI) under visible-light irradiation. However, it is reasonable to consider a deposition of Cr(III) species on the surface of TiO_2 nanoparticles during the photocatalytic oxidation of organics in the presence of Cr(VI) . This will result in the formation of Cr(III) -grafted TiO_2 as reported by

Table 1
The apparent rate constant k_{org} of organic pollutants over TiO_2 in the absence and presence of $0.1 \text{ mM Cr}_2\text{O}_7^{2-}$, and the calculated E_{HOMO} and VIP values for the tested organic compounds.

Organic pollutants	$k_{\text{org}} (10^{-3} \text{ min}^{-1})$		$E_{\text{HOMO}} (\text{eV})$	VIP (eV)
	Organics alone	Organics + Cr(VI)		
Benzoic acid	0.0	0.0 (-) ^a	-6.313	9.130
Phenol	0.46	1.3 (2.8)	-6.014	9.054
Aniline	0.18	1.2 (6.7)	-5.959	8.973
Terephthalic acid	0.0	0.0 (-)	-6.449	8.941
<i>p</i> -Hydroxybenzoic acid	0.36	1.2 (3.3)	-6.204	8.910
<i>p</i> -Aminobenzoic acid	0.38	1.1 (2.9)	-6.177	8.786
Salicylic acid	1.4	14 (10.0)	-5.769	8.550
8-Hydroxyquinoline	5.7	55 (9.7)	-5.306	7.940

^a The values in the parentheses are the ratio of k_{org} in the presence of Cr(VI) to that in the absence of Cr(VI).

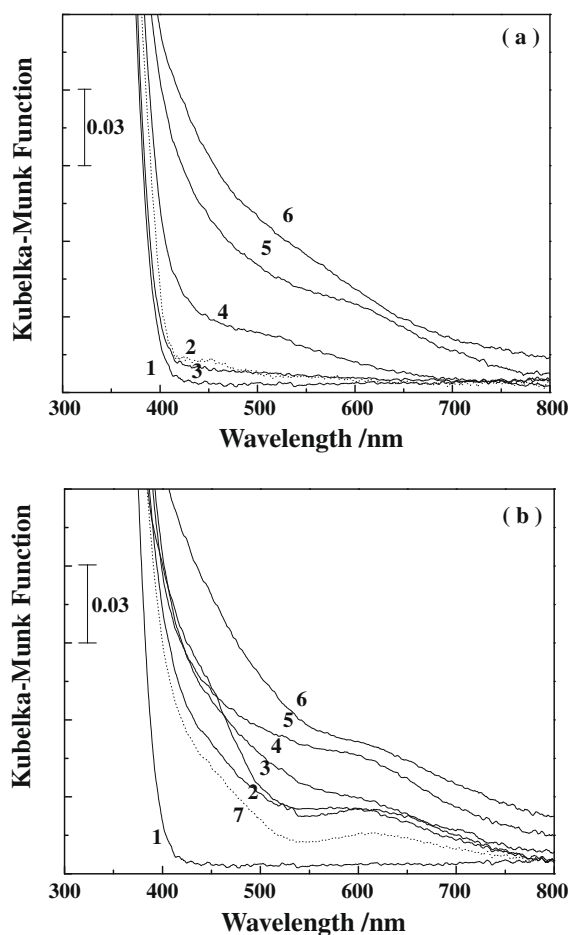
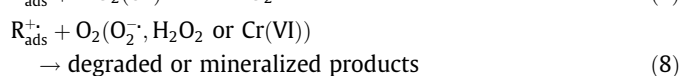
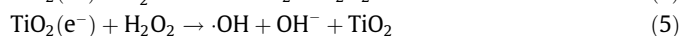
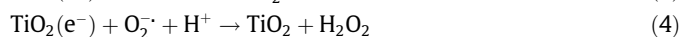
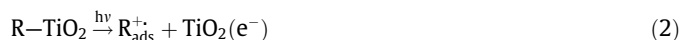


Fig. 2. DRS spectra of pollutant-adsorbed TiO_2 in the absence (a) and presence (b) of Cr(VI) for the pollutants of (2) aniline, (3) benzoic acid, (4) salicylic acid, (5) *p*-aminobenzoic acid, and (6) 8-hydroxyquinoline. The DRS spectra of TiO_2 (1) and Cr(VI)-adsorbed TiO_2 (7) are given as controls.

Irie et al. [28], which will make some contributions to CTC-mediated photocatalytic degradation of organics under visible-light irradiation.

3.2. Effects of chemical structure of pollutants on the CTC-mediated process

The CTC-mediated path for the photocatalytic degradation of the concerned colorless organic pollutants (R) can be simply represented as follows:



As discussed above, some of the colorless organic pollutants can be photocatalytically degraded under visible irradiation via the CTC-mediated path, but some others cannot; some are degraded fast, and some do slowly. This suggests that the chemical structure of the organic pollutants influences the CTC-mediated process. It is observed from Fig. 1 and Table 1 that the CTC-mediated degradation process does not occur for benzoic and terephthalic acids, which are two benzene derivatives with isolated carboxyl group, whereas the other tested aromatic organics containing hydroxyl group or amino group can be photodegraded under the visible irradiation. Especially, both salicylic acid and *p*-hydroxybenzoic acid have the same functional groups, but the photodegradation of the former is much faster than that of the latter. These hint that the nature of substituent groups and their positions play an important role in the proposed CTC-mediated process. Firstly, E_{HOMO} and VIP which are of particular important properties in the electron transfer are influenced strongly by the substituent. As shown in Table 1, the calculated E_{HOMO} is observed to increase in the order of terephthalic acid < benzoic acid < *p*-hydroxybenzoic acid < *p*-aminobenzoic acid < phenol < aniline < salicylic acid < 8-hydroxyquinoline, while the calculated VIP is decreased roughly in the same order. This is because an electron-donating substituent such as a hydroxyl or a amino group will raise the E_{HOMO} and lower the VIP of the parent organic pollutants, whereas the electron-withdrawing carboxyl groups have an opposite effect [30,31]. Secondly, the electron-donating effect on the increasing of the electron density of aromatic ring and the lowering of VIP will make the organic substrate easily oxidized [30]. Thus, by correlating k_{org} with E_{HOMO} and VIP of benzene derivatives, the quantitative relationships between structure and activity (QSAR) were obtained as the regression equations (Fig. 3): $1000 k_{\text{org}} = 30.2 + 4.8 E_{\text{HOMO}}$ ($R = 0.90$) and $1000 k_{\text{org}} = 42.9 - 4.8 \text{VIP}$ ($R = 0.95$). The QSAR demonstrates that the CTC-mediated process is mainly affected by the E_{HOMO} and VIP of organic molecules, namely, a high E_{HOMO} or low VIP is favorable to the electron transfer, thereby resulting in acceleration of the photodegradation of organics. Therefore, it is rational that the photodegradation rate of the tested organics increases in the

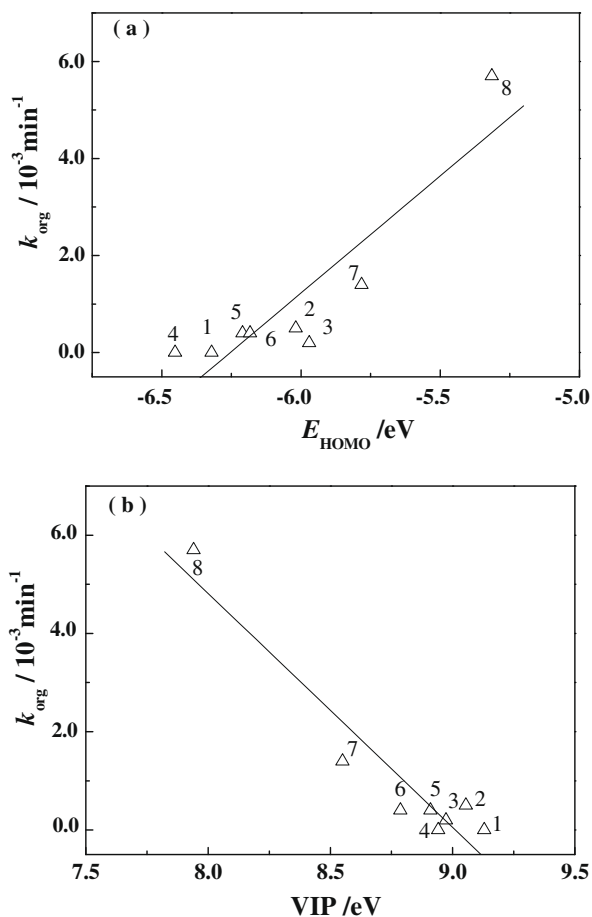


Fig. 3. Relationships between the apparent rate constant k_{org} and E_{HOMO} (a) or VIP (b) of the tested organic compounds. Numbers 1 to 8 represent benzoic acid, phenol, aniline, terephthalic acid, *p*-hydroxybenzoic acid, *p*-aminobenzoic acid, salicylic acid, and 8-hydroxyquinoline, respectively.

observed order of terephthalic acid, benzoic acid < *p*-hydroxybenzoic acid, *p*-aminobenzoic acid, phenol < salicylic acid < 8-hydroxyquinoline as shown in Table 1. Neither benzoic acid nor terephthalic acid can be degraded via a CTC-mediated pathway, because the former has the highest VIP and the latter has the lowest E_{HOMO} .

However, aniline seems to be an exception (Table 1 and Fig. 3). Amino group has a stronger electron-donating effect, causing greater E_{HOMO} -raising and VIP-lowering effect than hydroxyl group on the benzene ring (Table 1). Therefore, aniline should exhibit a faster reaction rate than phenol. Nevertheless, aniline ($k_{\text{org}} = 0.18 \times 10^{-3} \text{ min}^{-1}$) is more slowly degraded than phenol ($k_{\text{org}} = 0.46 \times 10^{-3} \text{ min}^{-1}$). It is ascribed to the weak interaction between aniline and TiO_2 surface because of the electrostatic repulsion between the positively charged surface of TiO_2 and the protonated aniline at pH 3.0 [32], which is evidenced by the little change in the DRS spectrum of TiO_2 when aniline is adsorbed (curve 2 in Fig. 2a). This means that besides the E_{HOMO} and VIP effects, a stronger interaction between the organic and TiO_2 surface is helpful to the electron transfer. The formation of surface complexes is a primary requisite and the effective electron transfer is an essential process for the photodegradation of colorless organics over pure TiO_2 under the visible irradiation. When aniline is substituted in the *para*-position by a carboxyl group, k_{org} of the resultant *p*-aminobenzoic acid is significantly increased to $0.38 \times 10^{-3} \text{ min}^{-1}$. Such a marked increase is attributed to the enhanced adsorption of *p*-aminobenzoic acid on TiO_2 via the carboxyl group,

which causes a fairly marked red shift into the visible region of the DRS spectrum (curve 4 in Fig. 2a), and also to the amino group which increases the electron density of the aromatic ring, raises E_{HOMO} and lowers VIP (Table 1), resulting in favorable charge separation between the adsorbed organics and TiO_2 CB. This is further confirmed by the fact that 8-hydroxyquinoline shows the highest photocatalytic degradation rate constant of $5.7 \times 10^{-3} \text{ min}^{-1}$ among the tested organics. As known, 8-hydroxyquinoline is more favorable to form a five-membered ring with titanium orbital and contains two electron donors where both N and O atoms can supply their unshared electron pair to pyridine and benzene rings, respectively. This results in the highest E_{HOMO} and the lowest VIP (Table 1), being consequently beneficial to enhance the electron transfer power and to accelerate the photodegradation.

3.3. Enhancing effect of sacrificial electron acceptors on the CTC-mediated degradation

Although the colorless organic pollutants with favorable chemical structures can be degraded over TiO_2 under visible irradiation via the CTC-mediated path, their degradation rates are slow for their removal from practical wastewaters. As we know, when the photoinduced electron of surface complex is injected into TiO_2 CB, it must be transferred to external electron acceptors, otherwise, it will recombine with the surface complex to make a null cycle [17,18]. Thus, the effects of external electron acceptors (such as O_2 , Cr(VI) , Cu^{2+} , BrO_3^- , and H_2O_2) were further investigated on the CTC-mediated photodegradation.

Dissolved O_2 is the commonest electron acceptor to suppress the charge recombination in photocatalytic systems. When N_2 was bubbled during the photocatalytic process, the degradation of salicylic acid was considerably inhibited as shown in Table 2, because of the O_2 depletion by the N_2 bubbling. Except Cu^{2+} , which drastically reduced the degradation rate of salicylic acid, the other electron scavengers significantly increased k_{org} of salicylic acid from $1.4 \times 10^{-3} \text{ min}^{-1}$ without any additive to 6.1×10^{-3} , 13.1×10^{-3} , and $14.0 \times 10^{-3} \text{ min}^{-1}$ for H_2O_2 , BrO_3^- and Cr(VI) , with a factor of 4.4, 9.4, and 10.0 times, respectively. Our observations are different from the findings reported by Kim and Choi [17] and Paul et al. [18], who observed that the addition of Fe^{3+} or BrO_3^- did not enhance the degradation of organics. This difference is possibly related to the much higher concentrations of electron acceptors (10 mM) in their work [17,18] than that (0.1 to 0.6 mM) in the present work, because the presence of much superabundant Fe^{3+} and/or BrO_3^- is unfavorable to the formation of CTC. It must be noted that no chemical reaction between the added electron acceptor and salicylic acid was observed in TiO_2 -free dispersions under visible irradiation (curve 5 in Fig. 1b, and Fig. S1 in Supporting information). When an appropriate amount of Cr(VI) was added, the role of dissolved oxygen became unimportant, and the N_2 bubbling did not influence the photocatalytic degradation of salicylic acid in the presence of Cr(VI) (Table 2). The addition of sacrificial electron acceptors promoted not only the photodegradation of salicylic acid but also its mineralization under visible irradiation. For

Table 2

The apparent rate constant k_{SA} of the degradation of salicylic acid (SA) over TiO_2 in the presence of different electron acceptors or superoxide dismutase (SOD).

Additive	$k_{\text{SA}} (10^{-3} \text{ min}^{-1})$	Additive	$k_{\text{SA}} (10^{-3} \text{ min}^{-1})$
Blank ^a	1.4	0.6 mM Cu^{2+}	0.32
0.3 mM H_2O_2	6.1	100 mg L^{-1} SOD	1.7
0.1 mM BrO_3^-	13.1	N_2 bubbling	0.10
0.2 mM Cr(VI)	14.0	$\text{N}_2 + 0.2 \text{ mM Cr(VI)}$	14.1

^a The blank condition represents the visible-light photocatalytic degradation of Salicylic acid (0.1 mM) over TiO_2 (1.0 g L^{-1}) in air-saturated suspensions at pH 3.0.

example, in the TiO₂ dispersions with salicylic acid alone, the total organic carbon (TOC) was decreased slowly by 22% within 5 h, whereas the presence of H₂O₂ and Cr(VI) decreased the TOC to 41% and 64% within 5 h, respectively (Fig. 4a). The little decrease of TOC in the presence of Cr(VI) beyond 3 h was attributed to the complete consumption of the added Cr(VI). Trace aromatic intermediates were detected by HPLC analysis (Fig. S2 in Supporting information), but the generation and accumulation of aliphatic acids such as formic acid are not negligible, as shown in Fig. 4b, indicating that by visible-light photocatalysis, salicylic acid can be converted to small aliphatic acids and then to CO₂ and H₂O. The accumulation of formic acid was low and was slightly increased with illumination time, due to the slow photodegradation of salicylic acid over TiO₂. When Cr(VI) or H₂O₂ was added, a higher and rapid accumulation of formic acid occurred, being ascribed to the enhancing effect of sacrificial electron acceptors on the salicylic acid degradation. Especially, H₂O₂ can be used as a green electron scavenger, and the produced ·OH radical (reaction 5) can effectively crack the benzene ring structure, because of its highly oxidative ability.

The enhancing effects of the sacrificial electron acceptors (such as Cr(VI)) on the CTC-mediated degradation were generally observed for other tested organic pollutants. It can be seen from Table 1 that the addition of Cr(VI) significantly enhances the photocatalytic degradation of the organics by a factor of 3 to 10 times, but the presence of Cr(VI) cannot induce any observable photocatalytic

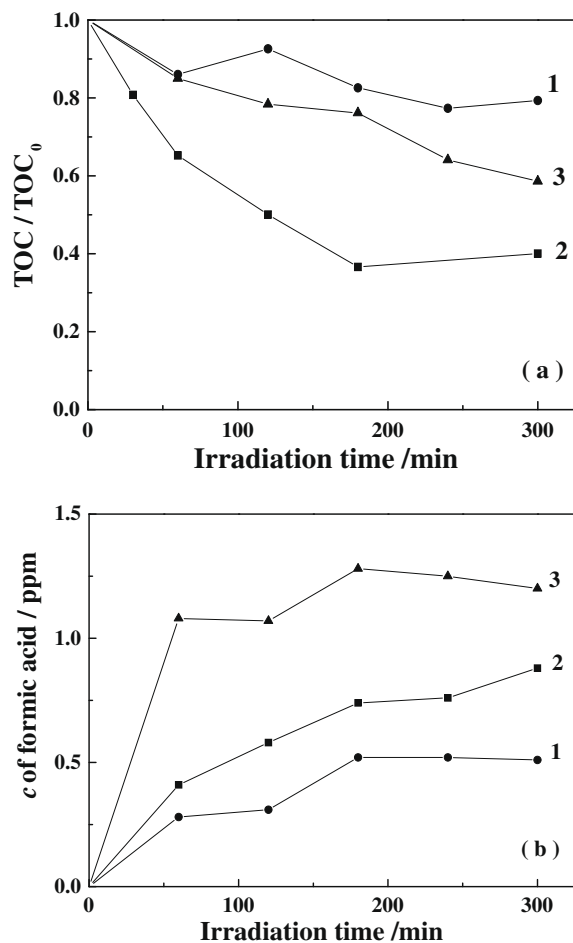


Fig. 4. Removal of TOC (a) and generation of formic acid (b) during the photocatalytic degradation of 0.1 mM salicylic acid (TOC₀ = 8.6 ppm) over TiO₂ in the absence (1, 1') and presence of 0.2 mM Cr(VI) (2, 2') and 0.3 mM H₂O₂ (3, 3') as electron acceptors.

degradation of benzoic acid and terephthalic acid, the degradation of which alone over TiO₂ is not detectable under visible irradiation. In addition, the presence of Cr(VI) almost does not change the order of the degradation rate constant of the organic pollutants. Although the DRS spectrum of Cr(VI)-adsorbed TiO₂ shows a broad band in the visible region (curve 7 in Fig. 2b), the adsorbed Cr(VI) cannot make the inherent TiO₂ be photo-excited by visible light,

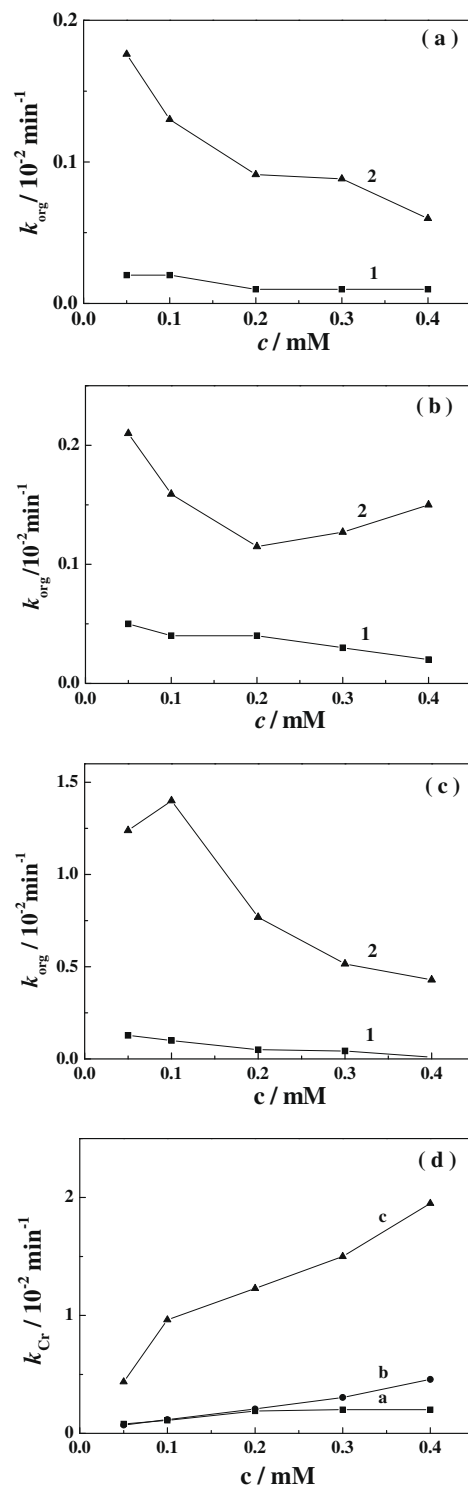


Fig. 5. Effects of initial concentration of organics on k_{org} of organic pollutants in the absence (1) and presence (2) of Cr(VI), and k_{Cr} of Cr(VI) conversion (d) for the organic systems of (a) aniline, (b) *p*-aminobenzoic acid, and (c) salicylic acid.

which is supported by the fact that no Cr(VI) photoreduction is observed in TiO₂ suspensions without organics after an irradiation of 5 h, due to the lack of photo-induced electron in TiO₂ CB. Thus, the fate of the electron trapped by Cr(VI) is triggered only by the charge transfer within the titanium(IV)-organics surface complexes, which is influenced mainly by the nature of organics as discussed above. In addition, the positive effect of Cr(VI) may be affected by the relative concentration of organics to Cr(VI) on TiO₂ surface, due to its double effects: competitive adsorption on the active sites of TiO₂ and trapping the injected electrons.

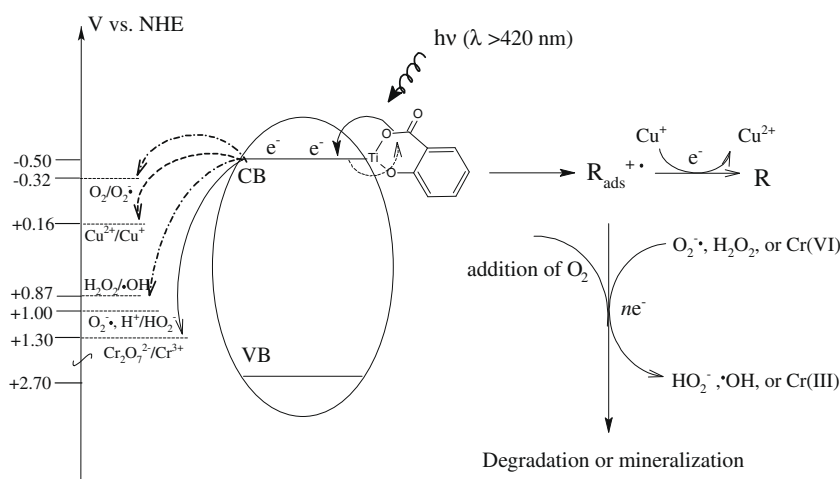
3.4. Effect of substrate concentration on the CTC-mediated degradation

Fig. 5 illustrates the dependence of visible-light photocatalytic degradation rate constant on the initial concentration of organic pollutants, where Cr(VI) was again selected to add into TiO₂ dispersions in consideration of the easy monitoring of the concentration variation of the added sacrificial electron acceptor. In the absence of Cr(VI), the photocatalytic degradation of all the tested organics is decreased slowly with increases in their initial concentrations, being consistent with the general observation that a low initial concentration of an organic compound is favorable to its photocatalytic degradation [33]. However, the addition of Cr(VI) enhances markedly the photooxidation of organics and changes the trends of k_{org} , which is dependent on initial concentration of organics. As the concentration of aniline was increased from 0.05 to 0.4 mM, its degradation rate constant was decreased from 1.8×10^{-3} to $0.59 \times 10^{-3} \text{ min}^{-1}$. For *p*-aminobenzoic acid, its k_{org} was decreased dramatically in the beginning up to about 0.2 mM and thereafter increased slightly. On the other hand, k_{org} of salicylic acid reaches a maximum at the initial concentration of 0.1 mM. These distinct trends of k_{org} in the presence of Cr(VI) are ascribed to a combination of different factors. As the initial concentration of organics is increased, the increased adsorption of organics on TiO₂ favors the intramolecular electron transfer within the surface complexes, whereas the amount of adsorbed Cr(VI) is diminished because of the competitive adsorption, which weakens the enhancing effect of Cr(VI) on the charge separation. However, the added aniline affects little on the adsorption of Cr(VI) because of its low affinity for TiO₂ surface, and the adsorbed *p*-aminobenzoic acid can drive the negatively charged Cr₂O₇²⁻ through the protonated amino group. Thus, the dependence of the degradation rate constant on the substrate concentration at a given addition amount of Cr(VI) also originates from the different chemical structures of organic pollutants.

The critical influence of the chemical structure of organic pollutant on the substrate concentration dependence of its degradation rate constant is further reflected by the photocatalytic reduction of the electron scavenger at different concentrations of organic pollutants. Along with the oxidation of the organics, the electron acceptor was reduced. For example, the conversion of the added 0.2 mM Cr(VI) achieves almost 100% over TiO₂ in the presence of 0.1 mM salicylic acid within 5 h illumination (curve 6 in Fig. 1b), indicative of a complete removal of the toxic Cr(VI). As shown in Fig. 5, the variation tendency for k_{Cr} value at different concentrations of the organic substrates is quite different when different organics are used as the substrate (curve 3 in Figs. 5a–c). At any given concentration of the organic substrates, the value of k_{Cr} is increased in the order of aniline < *p*-aminobenzoic acid < salicylic acid, which is well consistent with the order of the degradation rate constant (k_{org}) of the organic pollutants. In the mixture of the organic pollutant and the sacrificial electron scavenger, the overall photocatalytic process proceeds mainly via the simultaneous photooxidation of the organic pollutant and the photoreduction of the electron scavenger. The good consistence between the orders of k_{Cr} and k_{org} at a fixed concentration of Cr(VI) clearly demonstrates that the rate-determination step in the overall photocatalytic process is the photooxidation of the organic substrate, but not the photoreduction of the sacrificial electron scavenger. Therefore, the reduction of the sacrificial electron scavenger such as Cr(VI) is observed to be dependent on the chemical structure of the organic pollutant.

3.5. Reaction mechanisms

The above discussion demonstrates that some colorless aromatic organics such as phenolic and aniline compounds can be photodegraded slowly over pure TiO₂ under visible-light irradiation via a CTC-mediated path, and their photooxidation rates are significantly enhanced by adding proper sacrificial electron acceptors. The likely mechanisms for the TiO₂-assisted photodegradation of colorless organic pollutions in the absence and presence of a sacrificial electron acceptor are depicted in Scheme 1. In general, the photo-injected electrons in TiO₂ CB are rapidly delivered to pre-adsorbed O₂, producing O₂^{•-} and/or H₂O₂ that, together with O₂ molecules, play a key role in the removal of organic pollutants. Although the produced reactive oxygen species will be slowly desorbed into solution, it is highly likely that most primary reactions occur at the surface of TiO₂ particles. Accordingly, the photooxidation of organic pollutants is not affected by the added excess



Scheme 1. CTC-mediated mechanism for TiO₂-assisted photodegradation of colorless aromatic pollutants under visible irradiation.

radical scavengers such as 1.0 mM *tert*-butyl alcohols or even 100 mg L⁻¹ enzyme superoxide dismutase (SOD) which has little affinity for TiO₂ surface (Table 2). However, the O₂ reduction is limited by its slow adsorption rate on TiO₂ surface, because the adsorption requires the presence of surface defect sites [34]. Consequently, the recombination of the photo-injected electrons in TiO₂ CB with adsorbed R[•] radicals can complete effectively with the charge-trapping by loosing of O₂ on TiO₂ surface, and then the generated reactive oxygen species are diminished, thereby suppressing the photodegradation and mineralization of organic pollutants.

When another appreciate electron acceptor such as H₂O₂, BrO₃⁻ or Cr(VI) is added into TiO₂ suspensions, it can adsorb easily on TiO₂ surface via the electrostatic attraction or a coordination reaction [35], and then effectively trap the injected electrons in TiO₂ CB, resulting in the marked depression of the backward recombination event and the acceleration of the removal of pollutants. Moreover, another important reason is because the redox potentials of these electron acceptors ($E^{\circ}(\text{Cr}_2\text{O}_7^{2-}/\text{Cr}^{3+}) = 1.36 \text{ V}$, $E^{\circ}(\text{BrO}_3^-/\text{Br}^-) = 1.478 \text{ V}$, $E^{\circ}(\text{H}_2\text{O}_2/\cdot\text{OH}) = 0.87 \text{ V}$ vs NHE)) are more positive than the potential of R_{ads}[•] radicals (<1.0 V vs NHE), which means that the electron transfer from R_{ads}[•] to the used electron scavengers is thermodynamically feasible, leading to the oxidation of R_{ads}[•] radicals [14,26,33,36,37], and thereby a faster mineralization rate for salicylic acid was observed in the presence of Cr(VI) or H₂O₂. This alternative proposition is further supported by the inhibition effect of Cu²⁺ on the removal of salicylic acid (Table 2), being similar to its depressing effect on the photodegradation of dyes under visible irradiation [14]. Although, adsorbed Cu²⁺ can trap the injected electrons in TiO₂ CB, the charge recombination between the copper-induced surface state and the R_{ads}[•] radicals is possible, due to its low redox potential ($E^{\circ}(\text{Cu}^{2+}/\text{Cu}^+) = 0.159 \text{ V}$ vs NHE). Meanwhile, the reduction of O₂ is seriously hindered by the presence of Cu²⁺ as an electron scavenger. This subsequently blocks the formation of reactive oxygen species (O₂⁻, H₂O₂) [14,38], and suppresses the photodegradation of organic pollutants.

4. Conclusions

Neither pure TiO₂ nor the aromatic pollutants tested in the present work absorb visible light, but most of these organic pollutants can be photocatalytically degraded on pure TiO₂ under visible irradiation through a CTC-mediated path. It was found that either a higher E_{HOMO} or lower VIP favors the intramolecular charge transfer within surface complexes formed between the pollutant and TiO₂, consequently enhancing the photodegradation of the organic pollutants. The electron-withdrawing carboxyl group attenuates the electron density of aromatic ring, decreases E_{HOMO} and raises VIP, and thereby suppresses the charge transfer, resulting in no photodegradation of both benzoic acid and terephthalic acid. In contrast, the electron donors such as hydroxyl and amino groups provide a larger driving force for the electron transfer, favoring the photocatalytic degradation of the parent organic pollutants under the visible irradiation. The addition of electron acceptors such as H₂O₂ accelerated significantly both the photodegradation and

mineralization of the colorless organic compounds, which allow that the CTC-mediated photocatalytic degradation over TiO₂ to be applied for removing colorless organic pollutants under the visible irradiation.

Acknowledgment

Financial supports from the National Science Foundation of China (Grants Nos. 20877031 and 20677019) are gratefully acknowledged.

Appendix A. Supplementary data

Supplementary data associated with this article can be found, in the online version, at doi:10.1016/j.jcat.2009.06.006.

References

- [1] X. Shen, L. Zhu, G. Liu, H. Yu, H. Tang, *Environ. Sci. Technol.* 42 (2008) 1687.
- [2] D. Hufschmidt, D. Bahnemann, J.J. Testa, M.I. Litter, *J. Photochem. Photobiol. A: Chem.* 148 (2002) 223.
- [3] J.S. Jang, S.M. Ji, S.W. Bae, H.C. Son, J.S. Lee, *J. Photochem. Photobiol. A: Chem.* 188 (2007) 112.
- [4] J. Li, L. Zhu, Y. Wu, Y. Harima, A. Zhang, H. Tang, *Polymer* 47 (2006) 7361.
- [5] B. Sun, E.P. Reddy, P.G. Smirniotis, *J. Catal.* 237 (2006) 314.
- [6] A. Kubacka, M. Fernández-García, G. Colón, *J. Catal.* 254 (2008) 272.
- [7] X. Shen, L. Zhu, J. Li, H. Tang, *Chem. Commun.* (2007) 1163.
- [8] L. Wang, N. Wang, L. Zhu, H. Yu, H. Tang, *J. Hazard. Mater.* 152 (2008) 93.
- [9] S. Tojo, T. Tachikawa, M. Fujitsuka, T. Majima, *J. Phys. Chem. C* 112 (2008) 14948.
- [10] T. Tachikawa, M. Fujitsuka, T. Majima, *J. Phys. Chem. C* 111 (2007) 5259.
- [11] X. Yang, C. Cao, L. Erickson, K. Hohna, R. Maghirang, K. Klabunde, *J. Catal.* 260 (2008) 128.
- [12] X. Yang, C. Cao, K. Hohn, L. Erickson, R. Maghirang, D. Hamal, K. Klabunde, *J. Catal.* 252 (2007) 296.
- [13] G. Liu, X. Li, J. Zhao, H. Hidaka, N. Serpone, *Environ. Sci. Technol.* 34 (2000) 3982.
- [14] C. Chen, X. Li, W. Ma, J. Zhao, *J. Phys. Chem. B* 106 (2002) 318.
- [15] A.G. Agrios, K.A. Gray, E. Weitz, *Langmuir* 19 (2003) 1402.
- [16] A.G. Agrios, K.A. Gray, E. Weitz, *Langmuir* 20 (2004) 5911.
- [17] S. Kim, W. Choi, *J. Phys. Chem. B* 109 (2005) 5143.
- [18] T. Paul, P. Miller, T.J. Strathmann, *Environ. Sci. Technol.* 41 (2007) 4720.
- [19] M. Li, P. Tang, Z. Hong, M. Wang, *Colloid Surf. A* 318 (2008) 285.
- [20] G. Te Velde, F.M. Bickelhaupt, E.J. Baerends, C. Fonseca Guerra, S.J.A. Van Gisbergen, J.G. Snijders, T. Zeigler, *J. Comput. Chem.* 22 (2001) 931.
- [21] S.H. Vosko, L. Wilk, M. Nusair, *Can. J. Phys.* 58 (1980) 1200.
- [22] J.P. Perdew, K. Burke, *Int. J. Quant. Chem.* 57 (1996) 309.
- [23] H. Kyung, J. Lee, W. Choi, *Environ. Sci. Technol.* 39 (2005) 2376.
- [24] T. Papadam, N.P. Xekoukoulotakis, I. Poulou, D. Mantzavinos, *J. Photochem. Photobiol. A: Chem.* 186 (2007) 308.
- [25] A.E. Regazzoni, P. Mandelbaum, M. Matsuyoshi, S. Schiller, S.A. Bilmes, M.A. Blesa, *Langmuir* 14 (1998) 868.
- [26] S. Tunesi, M. Anderson, *J. Phys. Chem.* 85 (1991) 3399.
- [27] Y. Liu, J.I. Dadap, D. Zimdars, K.B. Esisenthal, *J. Phys. Chem. B* 103 (1999) 2480.
- [28] H. Irie, S. Miura, R. Nakamura, K. Hashimoto, *Chem. Lett.* 37 (2008) 252.
- [29] N. Wang, Y. Xu, L. Zhu, X. Shen, H. Tang, *J. Photochem. Photobiol. A: Chem.* 201 (2009) 21.
- [30] S.V. Jovanovic, S. Steeden, M. Tosic, B. Marjanovic, M.G. Simic, *J. Am. Chem. Soc.* 116 (1994) 4846.
- [31] J.S. Wright, E.R. Johnson, G.A. DiLabio, *J. Am. Chem. Soc.* 123 (2001) 1173.
- [32] A. Kumar, N. Mathur, *J. Colloid Interf. Sci.* 300 (2006) 244.
- [33] H.S. Hilal, L.Z. Majjad, N. Zaatat, A. El-Hamouz, *Solid State Sci.* 9 (2007) 9.
- [34] A.L. Linsebigler, G.Q. Lu, J.T. Yates, *Chem. Rev.* 95 (1995) 735.
- [35] C.S. Uyguner, M. Bekbolet, *Appl. Catal. B: Environ.* 49 (2004) 267.
- [36] M.I. Litter, *Appl. Catal. B: Environ.* 23 (1999) 89.
- [37] T. Hirakawa, Y. Nosaka, *Langmuir* 18 (2002) 3247.
- [38] N. Wang, Z. Chen, L. Zhu, X. Jiang, B. Lv, H. Tang, *J. Photochem. Photobiol. A: Chem.* 191 (2007) 193.